

THE UNIVERSITY OF CHICAGO

DATE September 16 19 49

Yeh, Tu-cheng

Author

Mar. 4, 1916

Birth Date

On Energy Dispersion in the Atmosphere

Title of Dissertation

Meteorology

Department or School

Ph.D.

Degree

December, 1948

Convocation

Permission is herewith granted to the University of Chicago to make copies of the above title, at its discretion, upon the request of individuals or institutions and at their expense.

T. 525 10-14-49

Date filmed

9

Number of pages

Tu cheng Yeh

Signature of author

T525

Extensive Quotation or Further Reproduction of This Material by Persons or Agencies Other than the University of Chicago May Not Be Made without the Express Permission of the Author.

SHORT TITLE: \_\_\_\_\_

IRREGULAR NUMBERING

OVERSIZED SHEETS

PAID { By cash   
By thesis deposit

DATE BILLED \_\_\_\_\_

2-25-49  
1

THE UNIVERSITY OF CHICAGO

ON ENERGY DISPERSION IN THE ATMOSPHERE

A DISSERTATION SUBMITTED TO  
THE FACULTY OF THE DIVISION OF THE PHYSICAL SCIENCES  
IN CANDIDACY FOR THE DEGREE OF  
DOCTOR OF PHILOSOPHY

DEPARTMENT OF METEOROLOGY

DECEMBER, 1948

BY

TU-CHENG YEH

Reprinted from

JOURNAL OF METEOROLOGY

Vol. 6, No. 1, February, 1949

## ON ENERGY DISPERSION IN THE ATMOSPHERE

By *Tu-cheng Yeh*

University of Chicago

(Manuscript received 27 April 1948)

### ABSTRACT

In this paper the energy propagation through dispersive waves in four atmospheric models is investigated. These waves are characterized by an approximate geostrophic balance. Diagrams showing the relation between group velocity, wave velocity, and wave length in the four types of atmosphere are given. It is found that:

1. In each of the four models there is always a range of wave length for which group velocity is larger than wave velocity, so that new waves can be formed ahead of initial waves.

2. Both divergence or convergence and horizontal solenoids give rise to waves with negative group velocity. But only in the presence of solenoids is there a range of wave length for which the speed of propagation of energy upstream is greater than the wave speed in the same direction. This means that only the horizontal solenoids make possible the formation of new waves upstream.

A graphical method is used to construct the distribution of phase resulting from an instantaneous point-source disturbance. The phase curves are constructed for each of the four atmospheric models.

Two applications of the theory are made. The formation of a new trough over North America following an intense cyclogenesis in the Gulf of Alaska is interpreted as a result of dispersion from a continuous point source of cyclonic relative vorticity into a previously straight westerly current. Computations show a pressure rise next to the region of cyclogenesis downstream and a trough farther to the east.

The blocking action observed in the west-wind belt is explained by the dispersion of an initial solitary wave. Calculations indicate that the life time of a "blocking action" is longer in high latitudes than in low latitudes; this is in agreement with observation.

### CONTENTS

1. Introduction.....	1
2. Wave length, phase velocity, and group velocity in different atmospheric models.....	2
3. The distribution of phase resulting from an instantaneous point-source disturbance.....	7
4. Formation of a new trough downstream from a region of cyclogenesis.....	10
5. Dispersion of an initial solitary wave; the blocking action and the intensity of disturbances at different latitudes.....	13
References.....	15

### 1. Introduction

Margulés (1905) first attempted to explain the origin of storm energy by conversion of potential energy into kinetic energy in a closed system. He obtained wind velocities of the correct order of magnitude to account for the kinetic energy of the storm from the release of potential energy of two air masses of different temperature standing side by side in a confined system. However, it is frequently observed that the kinetic energy and solenoidal energy increase at the same time in a cyclone. An excellent example has been given recently by Cressman (1948). A statistical investigation was made by Carson,<sup>1</sup> who found that an increase of the intensity of the solenoid field in the middle troposphere accompanied deepening

in about 80 per cent of the cases investigated. There exists, in fact, a considerable amount of evidence that strongly suggests the necessity of rejecting or modifying the concept of 'internal' or 'localized' transformations of the energy of certain characteristic atmospheric circulations, and that points to the need for investigating systematically the mechanisms of energy *transfer* in the atmosphere.

One such mechanism, and the most apparent, is the advective transport of energy, with the speed of the prevailing current. But energy can be transmitted without the help of advection. This paper is devoted to a study of the nonadvective transport of energy due to the rapid adjustment between pressure field and velocity field, a process which is a consequence mainly of the earth's rotation.

Namias (1944) has described the chain of events appearing downstream after sudden formation of an intense low in the Gulf of Alaska. The subsequent changes in circulation, which certainly cannot be explained by air-mass transport, provide an illustration of the process of rapid adjustment between pressure and velocity fields; we shall refer to the energy transmission resulting from this process as a *dispersive* transfer of energy.

The importance of dispersive processes in the atmosphere has recently been brought to the attention of meteorologists by Rossby (1945). Earlier (Rossby,

<sup>1</sup> J. E. Carson, "The variation of horizontal solenoidal concentration in the middle and low troposphere during cyclone formation," Master's thesis, University of Chicago, 1948.

1936) he had advanced the hypothesis that the horizontal pressure gradients observed in current systems of the atmosphere and the ocean to a large extent must be interpreted as reactions to the Coriolis forces impressed upon these systems by the rotation of the earth. He then showed (Rossby, 1937; 1938) that any sudden local addition of momentum to a rotating fluid body will initiate some type of inertia oscillation of that body. A small part of the initial energy goes into inertia oscillations, but the final equilibrium configuration set up between the pressure gradient and the current system is established in only a few pendulum hours. Part of the initial energy also goes into outlying portions of the fluid through dispersion by gravitational waves, as was demonstrated later by Cahn (1945), who gave a complete mathematical analysis of the problem. Through Rossby's work it is clear that a velocity field can result in a pressure field which in turn affects the velocity field. This is the physical mechanism of the dispersion process in the atmosphere.

Generally speaking, in a dispersive process the speed of propagation of energy is different from that of the prevailing current. The energy is propagated with the group velocity which, in the one-dimensional case, can be expressed in terms of phase velocity or wave length. A simple synoptic manifestation of dispersion is the common observation that a downstream pressure rise (or fall) usually follows an upstream pressure fall (or rise).

In this paper we shall investigate the role of dispersion in certain observed phenomena in the atmosphere. Before entering into a detailed discussion the following point should be noted. Dispersion arises from unbalanced motion. Once equilibrium is reached dispersion will cease. As pointed out above, dispersion essentially arises from the *tendency* for mutual adjustments between the pressure and velocity fields, but when these two fields are in balance dispersion ceases.

## 2. Wave length, phase velocity, and group velocity in different atmospheric models

The close relation between energy propagation and group velocity may be explained as follows. By group velocity we mean the velocity of a group of waves as a whole. The individual waves which compose this group may advance through it or may be left behind it, while the place of the individual wave in the group is occupied in succession by other waves. If we assume that the energy of wave motion is concentrated at the crests of the wave groups, the velocity of propagation of energy will certainly be associated with the group velocity. Group velocity, phase velocity, and wave length are related by the well-known formula

$$G = C - L dC/dL, \quad (1)$$

where  $G$  is the group velocity,  $C$  the phase velocity, and  $L$  the wave length.

In the atmosphere and the ocean almost all forms of wave motion are dispersive, *i.e.*, the phase velocity of individual waves depends on their wave length. The speed of energy propagation in such systems is usually different from that of the individual waves. Whether new waves will be formed ahead or in the rear of an initial wave train, or whether an increasingly long trailing wave train may develop, depends on the speed of propagation of energy. Since the energy propagation depends on group velocity which in turn is determined by wave length and phase velocity, a discussion of these three elements in different atmospheric models is desirable.

We shall consider in turn four atmospheric models:

*Model A:* A uniform, incompressible atmosphere of infinite depth, or of finite depth with a rigid cover.

*Model B:* A uniform, incompressible atmosphere with a free surface.

*Model C:* An incompressible atmosphere with a uniform north-south density gradient and a rigid cover.

*Model D:* An incompressible atmosphere with a uniform north-south density gradient and a free surface.

In each of these models there is a basic current with uniform and constant velocity  $U$ .

*Model A.*—The first model is the simplest and has been studied by Rossby (1939) and later by Haurwitz (1940). In this atmosphere divergence and convergence are absent, and for small one-dimensional motion the vorticity equation may be written as follows:

$$\frac{\partial^2 v}{\partial x \partial t} + U \frac{\partial^2 v}{\partial x^2} + \beta v = 0, \quad (2A)$$

where  $v$  is the perturbation velocity transverse to the  $x$ -direction, and  $\frac{1}{2}\beta$  represents the rate of change northward of the vertical component of the earth's angular velocity. Assuming a solution of the form  $e^{i(kx - \nu t)}$  the frequency equation from (2A) is  $\nu/k = U - \beta/k^2$ , where  $\nu$  is the frequency and  $k$  the wave number, or

$$C = U - \beta L^2, \quad (3A)$$

where  $C = \nu/k$  is the phase velocity and  $L = 1/k$  the wave length.<sup>2</sup> The group velocity, from (1), is then

$$G = U + \beta L^2. \quad (4A)$$

In this atmosphere the group velocity  $G$  is always positive and larger than the phase velocity  $C$ . It has a minimum value  $U$  and increases with wave length

<sup>2</sup> For simplicity in notation we shall depart from the usual convention of defining the wave length as  $2\pi/k$ . Thus  $L$ , as used throughout this paper, is equal to the 'conventional' wave length divided by  $2\pi$ .

(fig. 1). Since  $G$  is always positive and larger than  $U$ , the energy is always propagated downstream with a speed larger than  $C$ . In this system new waves will be formed ahead of initial waves.

*Model B.*—Removing the rigid cover from the first model we obtain the second type of atmosphere. In this model divergence and convergence are possible. The vorticity equation will then take the form

$$\frac{d}{dt} \left( \frac{f + \zeta}{D} \right) = 0,$$

where  $D$  is the depth of the atmosphere,  $\zeta$  the relative vorticity, and  $f$  the Coriolis parameter. Assuming the north-south motion to be geostrophic<sup>3</sup> and perturbations to be small, the vorticity equation may be written in the expanded form

$$\frac{\partial^3 D'}{\partial x^2 \partial t} + U \frac{\partial^3 D'}{\partial x^3} + \beta \frac{\partial D'}{\partial x} - \lambda^2 \frac{\partial D'}{\partial t} = 0, \quad (2B)$$

where  $\lambda^2 \equiv f^2/gD_0$ ,  $D_0$  is the undisturbed depth, and  $D'$  the deformation of the free surface. The wave velocity is

$$C = \frac{U - \beta L^2}{1 + \lambda^2 L^2}, \quad (3B)$$

and the group velocity may be obtained by substituting (3B) in (1), the result being

$$G = \frac{U + \beta L^2 + 2\lambda^2 L^2 C}{1 + \lambda^2 L^2}. \quad (4B)$$

The graphs for  $C$  and  $G$  are shown in fig. 2. The solid curve is the wave velocity  $C$ , obtained from (3B); the dashed curve is the group velocity  $G$ , from (4B). Both  $C$  and  $G$  have the same lower limit  $-\beta/\lambda^2$ , corresponding to infinite wave length. Thus the phase velocity  $C$  decreases with increasing wave length asymptotically to the limiting value  $-\beta/\lambda^2$ , not as in the nondivergent case where it decreases without limit. At the wave length  $L_s \equiv \sqrt{U/\beta}$  corresponding to zero phase velocity,

$$G = G_s \equiv 2U/(1 + \lambda^2 L_s^2).$$

The group velocity  $G$  first increases with wave length until the latter reaches a value where  $d^2C/dL^2 = 0$ ; at this point

$$G = G_{\max} \equiv \frac{1}{8}(9U + \beta\lambda^{-2})$$

$$C = \frac{3}{16}(3U - \beta\lambda^{-2}).$$

After this wave length is reached, the group velocity decreases first rapidly and then asymptotically to the value  $-\beta/\lambda^2$ .

<sup>3</sup> The geostrophic assumption results simply in the omission of long gravitational waves, in which we are not interested (Charney, 1947). The approximation of using the geostrophic relation after the vorticity equation has been written down does not mean that acceleration terms are neglected. The analysis of phase and group velocity in model B has been presented in Prof. Rossby's lectures and is reproduced here with his kind permission.

A striking difference between the nondivergent case and the present one in which convergence and divergence appear, is that in the latter the group velocity can be negative. This means that in divergent motion energy can be propagated upstream. Specific examples of this process will be given later. From fig. 2 it is seen that the group velocity is always larger than the phase velocity. Hence new waves may be formed downstream ahead of the initial disturbance, but not upstream in the rear of the initial disturbance, though energy can be propagated upstream. Since  $G = C$  for  $L \rightarrow \infty$ , energy will be propagated with the speed of these long retrogressive waves which may therefore retrograde without changing in intensity.

The particular interest of this model lies in the second group of waves, long and retrogressive with negative group velocity. The limiting value of this negative phase or group velocity is  $-\beta/\lambda^2$ , as already noted. These very long waves are nondispersive waves and move with practically constant relative vorticity. The change of vorticity due to latitude is balanced by the effect of divergence, as is easily seen from (2B). For very long wave length the first two terms in (2B) may be neglected since they are inversely proportional to the square or cube of wave length. Then the remaining two terms—expressing respectively the vorticity change produced by latitude variation and by divergence—must balance each other:

$$\partial D'/\partial t - \beta\lambda^{-2}\partial D'/\partial x = 0,$$

giving a phase velocity equal to  $-\beta/\lambda^2$ . Taking representative values in middle latitudes we find that  $-\beta/\lambda^2$  is of the order of 100 m sec<sup>-1</sup>. However, this unrealistically large value can never occur in the atmosphere due to the fact that the wave length is limited by the circumference of the earth.<sup>4</sup>

*Model C.*<sup>5</sup>—To investigate the effect of horizontal solenoids in purely horizontal motion we may imagine an infinitely deep atmosphere which has uniform density vertically and a uniform north-south density gradient. In this model convergence and divergence are absent, and the vorticity equation is

$$\frac{\partial^2 v}{\partial x \partial t} + U \frac{\partial^2 v}{\partial x^2} + \beta v = -\frac{\partial \alpha}{\partial x} \frac{\partial p}{\partial y} + \frac{\partial \alpha}{\partial y} \frac{\partial p}{\partial x} \equiv n,$$

$\alpha$  being the specific volume,  $p$  the pressure, and  $n$  the number of solenoids per unit area. For the purpose of

<sup>4</sup> The reduction of the unrealistically large value of the maximum negative group velocity was suggested by J. Charney.

<sup>5</sup> It should be noted that the two following atmospheric models, C and D, are not selfconsistent. In these two models the presence of horizontal stratification implies that the basic current  $U$  must increase with height, so the assumption of constant  $U$  is not justified. However, in the present paper we are concerned only with one level. As long as vertical motion does not appear (in model C) there may not be interference between upper and lower layers and thus it may be justified to deal with one level only; but in model D, vertical motion will be present and the analysis of this model is therefore only an approximation.

evaluating  $n$  it is reasonable to substitute the geostrophic wind relation;<sup>6</sup> one then obtains

$$\frac{\partial^2 v}{\partial x \partial t} + U \frac{\partial^2 v}{\partial x^2} + \beta v = f \left( \frac{dq}{dt} - \frac{\partial q}{\partial t} \right),$$

where  $q \equiv \ln \alpha$ . Since the motion is incompressible and horizontal we have

$$\frac{dq}{dt} = \frac{\partial q}{\partial t} + U \frac{\partial q}{\partial x} + v \frac{\partial q}{\partial y} = 0.$$

Writing  $s \equiv -\partial q/\partial y$  for the undisturbed value of the horizontal stratification, and assuming perturbations independent of  $y$ , the vorticity equation becomes

$$\frac{\partial^2 v}{\partial x \partial t^2} + 2U \frac{\partial^2 v}{\partial x^2 \partial t} + U^2 \frac{\partial^2 v}{\partial x^3} + (\beta + fs) \frac{\partial v}{\partial t} + \beta U \frac{\partial v}{\partial x} = 0. \quad (2C)$$

Assuming a solution of the form  $e^{i(kx - \nu t)}$  the wave velocity  $C = \nu/k$  is found to be

$$C = U - \frac{1}{2} \sigma L^2 (1 \pm l), \quad (3C)$$

where  $\sigma \equiv \beta + fs$ ,  $l \equiv (1 - L_c^2/L^2)^{1/2}$ , and  $L_c \equiv 2\sqrt{fsU}/\sigma$ . This is exactly the same result as derived by Jaw (1946) using a different approach. The group velocity corresponding to (3C) is

$$G = U + \frac{1}{2} \sigma L^2 (1 \pm l^{-1}). \quad (4C)$$

Equation (3C) reveals immediately one important aspect of this model, *i.e.*, there exists a critical wave length  $L_c$  below which  $C$  becomes complex. This implies the existence of unstable waves in this type of atmosphere. The instability increases with  $s$  and  $U$ . (It is easy to see that the instability increases with  $s$ . It increases with  $U$  because the isobaric slope is proportional to  $U$  and so also is the number of horizontal solenoids per unit area.) These unstable waves are relatively short and progressive.

There are two solutions for  $C$  corresponding to the two signs in the parenthesis of (3C). For  $L < L_c$ , the positive sign represents a damped wave system, while the negative sign represents unstable waves. Whether we choose the positive or negative sign (or both) is dependent on the type of boundary or initial conditions imposed on the disturbance. The wave system may therefore be unstable for certain types of disturbances and damped for other types. When  $L > L_c$  the waves are neutral, for either choice of sign in (3C).

*Damped or unstable waves.* For wave lengths smaller than the critical one the disturbance will be either damped or unstable. In either case  $C$  is a complex

number. The wave velocity will be the real part of (3C):

$$C = U - \frac{1}{2} \sigma L^2, \quad \text{for } L < L_c,$$

and the group velocity is

$$G = U + \frac{1}{2} \sigma L^2, \quad \text{for } L < L_c.$$

Thus  $G$  is always larger than  $C$  for this range of wave length. At the critical wave length,

$$G \rightarrow G_c \equiv U(1 + 2fs/\sigma), \quad \text{for } L \rightarrow L_c.$$

*Neutral waves.* When the wave length is larger than the critical value, we may take either the positive sign or the negative sign or both in (3C), depending on the nature of the disturbance. For simplicity we will consider the first two possibilities only.

Taking the positive sign in (3C), it is readily seen that

$$C \rightarrow C_c \equiv U(1 - 2fs/\sigma), \quad \text{for } L \rightarrow L_c;$$

and  $C \rightarrow -\infty$ , for  $L \rightarrow \infty$ . Differentiating (3C) with respect to  $L$  we have (for  $L > L_c$ )

$$dC/dL = -\frac{1}{2} \sigma L(l + 2 + l^{-1}),$$

which approaches negative infinity as  $L \rightarrow L_c$ , since  $l \rightarrow 0$ . The relation between group velocity and wave length is given by (4C) with plus sign. At the stationary wave length  $L_s$ , which can be seen to be equal to  $\sqrt{U/\beta}$ ,

$$G \rightarrow G_s \equiv 2\beta U/(\beta - fs), \quad \text{for } L \rightarrow L_s.$$

Also,  $G \rightarrow \infty$  as  $L \rightarrow L_c$  or  $L \rightarrow \infty$ . Hence, the group velocity will first decrease with increasing wave length until the minimum value  $G_{\min} \equiv U(1 + 8fs/\sigma)$  is reached, and then increases without limit. The curves for wave velocity and group velocity are shown in fig. 4. The solid curve represents wave velocity and the dashed curve group velocity; both curves have a distinct discontinuity at  $L = L_c$ .

Now let us consider the negative sign in the parenthesis of (3C), for the case  $L > L_c$ . It is readily seen that

$$\begin{aligned} C \rightarrow C_c &\equiv U(1 - 2fs/\sigma), & \text{for } L = L_c \\ C \rightarrow C_\infty &\equiv U(1 - fs/\sigma), & \text{for } L \rightarrow \infty. \end{aligned}$$

Further,  $dC/dL \rightarrow \infty$  as  $L \rightarrow L_c$ . Thus  $C$  increases very rapidly from  $C_c$  and then asymptotically to  $C_\infty$  as wave length further increases (fig. 3).

The expression for group velocity is given by (4C) with the minus sign, from which,

$$G \rightarrow G_\infty \equiv U(1 - fs/\sigma), \quad \text{for } L \rightarrow \infty,$$

and  $G \rightarrow -\infty$  as  $L \rightarrow L_c$ . From the curve for  $C$  it is seen that  $C$  increases first very rapidly and then asymptotically to  $G_\infty$ . The curves for  $C$  and  $G$  are

<sup>6</sup> See footnote 2.

shown in fig. 3, solid line for  $C$  and dashed line for  $G$ . Both curves are discontinuous at  $L = L_c$ . One interesting point is that no stationary wave length exists for this case; all waves are progressive. Since  $G \rightarrow C$  as  $L$  increases, long individual waves can travel downstream without changing intensity.

For the first type of disturbance—positive sign in (3C), damped waves for  $L < L_c$ —energy can be propagated only downstream. Since group velocity is larger than wave velocity new waves can be formed ahead of initial wave trains. For the second type of disturbance—negative sign in (3C), unstable waves for  $L < L_c$ —energy can be propagated in both directions. Since the speed of energy propagation in either direction can be larger in magnitude than the wave speed, new waves may be formed both downstream and upstream.

*Model D.*—We come now to the fourth and last model, in which both horizontal solenoids and divergence or convergence are operating. The vorticity equation in this case may be written:

$$\frac{d}{dt}(f + \zeta) = \frac{f + \zeta}{D} \frac{dD}{dt} + n.$$

For small motions we have

$$\frac{\partial^2 v}{\partial x \partial t} + U \frac{\partial^2 v}{\partial x^2} + \beta v + f \frac{\partial q}{\partial t} - \frac{f}{D_0} \frac{\partial D'}{\partial t} = 0.$$

In writing the above equation the geostrophic-wind relation was used in evaluating the divergence and solenoid terms of the vorticity equation.<sup>7</sup>

The geostrophic-wind equation for the north-south velocity component is

$$v = \frac{g}{f} \frac{\partial D}{\partial x},$$

and the condition for incompressibility is

$$\frac{\partial q}{\partial t} + U \frac{\partial q}{\partial x} = sv.$$

Through elimination of  $D'$  and  $q$  we have

$$\begin{aligned} \frac{\partial^4 v}{\partial x^2 \partial t^2} + 2U \frac{\partial^4 v}{\partial x^3 \partial t} + U^2 \frac{\partial^4 v}{\partial x^4} - \lambda^2 \frac{\partial^2 v}{\partial t^2} \\ + \beta U \frac{\partial^2 v}{\partial x^2} + b \frac{\partial^2 v}{\partial x \partial t} = 0. \end{aligned} \quad (2D)$$

where  $\lambda^2 \equiv f^2/gD_0$  and  $b \equiv \beta + fs - \lambda^2 U$ . Assuming a disturbance of wave form  $e^{i(kx - \omega t)}$  the phase speed  $C$  is found to be

$$C = \frac{U - \frac{1}{2}L^2(b \pm la)}{1 + \lambda^2 L^2}, \quad (3D)$$

where  $l \equiv (1 - L_c^2/L^2)^{1/2}$ ,  $a \equiv (b^2 + 4\beta\lambda^2 U)^{1/2}$ , and  $L_c \equiv 2\sqrt{fsU}/a$  is the critical wave length below which  $C$  becomes complex. It can be verified that (3D) reduces to equation (3B) by putting  $s = 0$  and goes to (3C) by putting  $\lambda^2 = 0$  (or  $gD_0 \rightarrow \infty$ ). The group velocity corresponding to (3D) is

$$G = \frac{U + \frac{1}{2}L^2(b \pm l^{-1}a) + 2\lambda^2 L^2 C}{1 + \lambda^2 L^2}. \quad (4D)$$

*Damped or unstable waves.* The wave velocity and group velocity have a discontinuity at  $L = L_c$  as in model C. When  $L < L_c$  we may take the wave velocity to be the real part of (3D) as before:

$$C = \frac{U - \frac{1}{2}bL^2}{1 + \lambda^2 L^2}.$$

It decreases with increase of  $L$ . For the group velocity we have, from (3D),

$$G = \frac{U + \frac{1}{2}bL^2 + 2\lambda^2 L^2 C}{1 + \lambda^2 L^2}.$$

This is always positive and larger than  $C$ .

*Neutral waves.* For  $L > L_c$  we take first the case of positive sign in (3D). As  $L$  increases,  $C$  will first decrease very rapidly and then asymptotically to its limiting negative value; thus

$$C \rightarrow C_\infty \equiv -\frac{1}{2}\lambda^{-2}(b + a), \quad \text{for } L \rightarrow \infty.$$

The group velocity (plus sign in (4D)) approaches positive infinity for  $L \rightarrow L_c$ , and decreases very sharply to a minimum value at approximately  $L = 0.9L_c$ . It increases again from this wave length to a maximum value at approximately  $L = 2.3L_c$  and then decreases to its asymptotic value  $G_\infty = C_\infty$  for  $L \rightarrow \infty$ . Fig. 5 shows the curves for  $C$  and  $G$  in relation to  $L$ .

Taking the negative sign in (3D), we can see that  $dC/dL \rightarrow \infty$  as  $L \rightarrow L_c$  and that

$$C \rightarrow C_\infty \equiv -\frac{1}{2}\lambda^{-2}(b - a), \quad \text{for } L \rightarrow \infty.$$

Thus,  $C$  first increases rapidly and asymptotically to the limiting value  $C_\infty$ . The group velocity (minus sign in (4D)) approaches negative infinity as  $L \rightarrow L_c$  and grows very rapidly to its maximum value (which is only very slightly higher than  $C_\infty$ ) and then gradually falls off to a limiting value  $G_\infty = C_\infty$  as  $L \rightarrow \infty$  (fig. 6).

In the first case of this model—positive sign in (3D), damped waves for  $L < L_c$ —new waves can be formed both upstream and downstream. Since  $G \rightarrow C > 0$  as  $L$  increases, long progressive waves can travel without changing intensity. In the second case—negative sign in (3D), unstable waves for  $L < L_c$ —new waves can be formed only downstream.

<sup>7</sup> See footnote 2.

In this case energy can be propagated upstream, but only for very long waves can energy travel with the individual waves, which then will not change in intensity.

It is interesting to compare figs. 1, 2, 4, and 5. In fig. 1 there is only one branch of waves, with only positive group velocity; the phase velocity decreases without limit while the group velocity increases without limit as wave length increases. The effect of divergence (fig. 2) is to add another branch of waves and to give rise to waves with negative group velocity. In the presence of divergence the magnitudes of the group and phase velocity are limited.

Comparing figs. 1 and 4 we see that the presence of solenoids also gives rise to another branch of waves, but the group velocity of this branch (from  $G_c$  to  $G_{min}$ ) is also positive. The combined effect of divergence and solenoids is clearly shown in fig. 5. Both  $G_{max}$  of fig. 2 and  $G_{min}$  of fig. 4 appear in fig. 5, as well as the effect of divergence in limiting the magnitude of the group and phase velocity ( $C \rightarrow G_x$  and  $G \rightarrow G_x$  as  $L \rightarrow \infty$ ).

We may call the branch of waves which appears in each of the four models the 'barotropic-nondivergent' branch, the branch of waves which appears only in the presence of divergence the 'divergent' branch, and the branch of waves which appears only in the presence of solenoids the 'solenoidal' branch. With this terminology<sup>8</sup> we can see that in fig. 1 we have only the barotropic-nondivergent branch. In fig. 2 the waves with wave length smaller than  $L_{max}$  (where  $G = G_{max}$ ) belong to the barotropic-nondivergent branch, while for wave lengths larger than  $L_{max}$  the waves belong to the divergent branch. In fig. 4 the waves with wave length between  $L_c$  and  $L_{min}$  (where  $G = G_{min}$ ) are of the solenoidal branch; all other wave lengths in this model may be considered to belong to the barotropic branch. In fig. 5 the solenoidal branch is between the wave length  $L_c$  and  $L_{min}$ , the divergent branch corresponds to wave length larger than  $L_{max}$  and the barotropic-nondivergent branch consists of waves of wave length smaller than  $L_c$  and between  $L_{min}$  and  $L_{max}$ .

If we consider figs. 3 and 6, we cannot separate the divergent from the solenoidal branch. In these two figures, only waves with wave length smaller than  $L_c$  are of barotropic-nondivergent character.

From the foregoing discussion we may note that the divergence affects mainly the long waves, that the solenoids affect mainly the waves of moderate wave length, and that the very short waves are not appreciably affected by either of these factors.

The foregoing analysis for models C and D was based on the assumption that the temperature gra-

dient is not very strong so that  $fs < \beta$ . For a temperature gradient strong enough so that  $fs > \beta$  the analysis must be modified somewhat.

Let us discuss model C first. The wave velocity for this model, when the wave length is smaller than the critical one, is

$$C = U - \frac{1}{2}\sigma L^2, \quad \text{for } L < L_c,$$

where  $\sigma \equiv \beta + fs$ . The stationary wave length for this range is

$$L_s' \equiv \sqrt{2U/(\beta + fs)}.$$

This is easily verified to be larger than, equal to, or smaller than the critical wave length  $L_c$  according as  $fs$  is smaller than, equal to, or larger than  $\beta$ . Hence there will not be a stationary wave in the region  $L < L_c$  if  $fs < \beta$ . In case  $fs > \beta$  there will then exist two stationary waves of wave lengths  $L_s' \equiv \sqrt{2U/(\beta + fs)}$  and  $L_s \equiv \sqrt{U/\beta}$  respectively in the regions  $L < L_c$  and  $L > L_c$ . If  $fs > \beta$ , it can be seen that both stationary waves will occur in fig. 4 while only the stationary wave of wave length  $L_s'$  will occur in fig. 3.

By differentiating the expression for  $L_c$  with respect to  $fs$  we obtain a maximum value of  $L_c$  for  $fs = \beta$ . This maximum value of  $L_c$  is equal to  $\sqrt{U/\beta}$ . Hence the value of  $L_c$  will always stay between  $L_s' \equiv \sqrt{2U/(\beta + fs)}$  and  $L_s \equiv \sqrt{U/\beta}$ . The three wave lengths, namely,  $L_s'$ ,  $L_c$ , and  $L_s$  will coincide when  $fs = \beta$ .

A similar discussion can also be applied to model D, the critical temperature gradient in this model being given by  $fs = \beta + \lambda^2 U$ .

The inequalities  $fs > \beta$  or  $fs > \beta + \lambda^2 U$  will not occur in lower latitudes, but may be valid in high latitudes where  $\beta$  is small and  $f$  is large, or in high elevations where the temperature gradient is strong. The existence of this secondary stationary wave length in the unstable (or damping) range of wave length may provide an explanation of the fact that a system frequently develops (or damps out) without displacement.

To summarize the discussion in this section we may make the following statements:

1. In each of the four models we have studied there is always a range of wave length for which the group velocity is larger than the wave velocity, so that new waves can be formed ahead of initial waves.

2. The presence of divergence or convergence reduces the speed of propagation of energy and gives rise to a barotropic-divergent branch of waves. The presence of horizontal solenoids gives rise to the solenoidal branch of waves and may produce two stationary wave lengths.

3. Both divergence or convergence and horizontal solenoids give rise to waves with negative group velocity. But only in the presence of solenoids is there a range

<sup>8</sup> The terms are not rigorous because the effect of divergence or solenoids does show up in the barotropic-nondivergent branch of waves of models C and D.



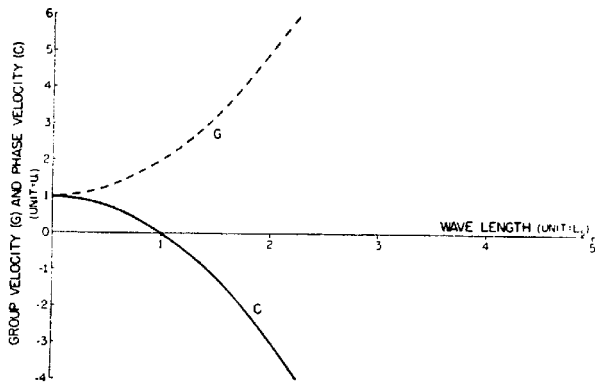


FIG. 1. Group velocity (broken line) and phase velocity (solid line) as a function of wave length in model A.

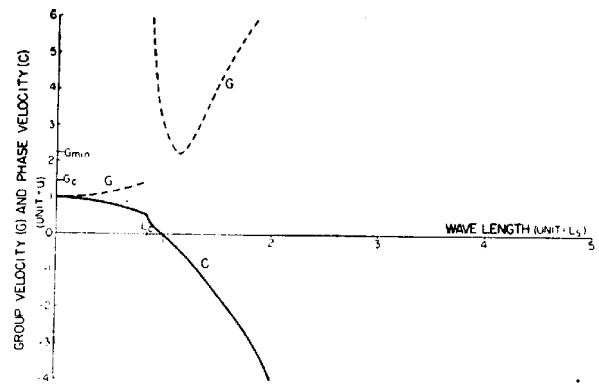


FIG. 4. Group velocity and phase velocity as a function of wave length in model C when the waves with wave length below the critical value  $L_c$  are damped (positive sign in eq. (3C)).

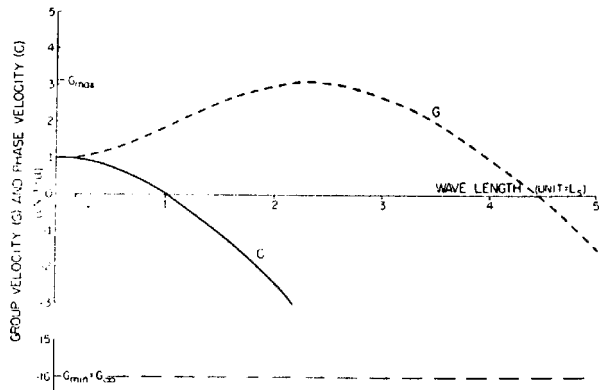


FIG. 2. Group velocity and phase velocity as a function of wave length in model B. Both curves are limited by the horizontal asymptotic line  $G_{\infty} = G_{min}$ .

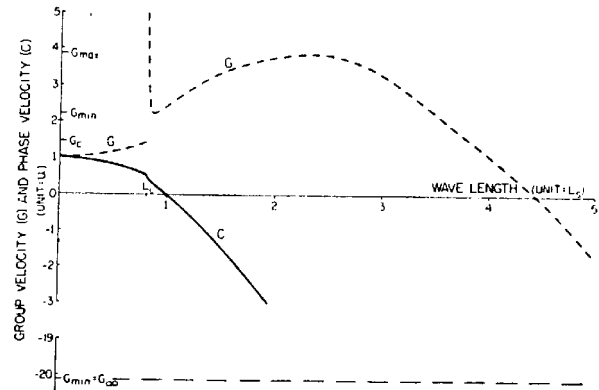


FIG. 5. Group velocity and phase velocity as a function of wave length in model D when the waves with wave length below the critical value  $L_c$  are damped (positive sign in eq. (3D)). Both curves are limited by the horizontal asymptotic line  $G_{\infty} = G_{min}$ .

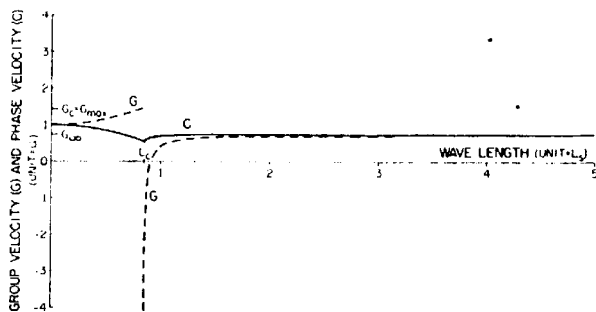


FIG. 3. Group velocity and phase velocity as a function of wave length in model C when the waves with wave length below the critical value  $L_c$  are unstable (negative sign in eq. (3C)).

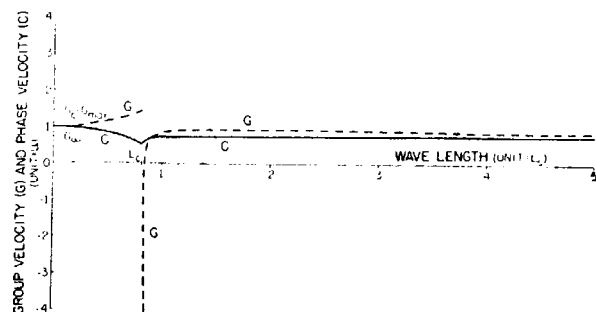


FIG. 6. Group velocity and phase velocity as a function of wave length in model D when the waves with wave length below the critical value  $L_c$  are unstable (negative sign in eq. (3D)).

of wave length for which the speed of propagation of energy upstream is greater than the wave speed in the same direction. This means that *only the horizontal solenoids make possible the formation of new waves upstream.*

### 3. The distribution of phase resulting from an instantaneous point-source disturbance

It is well known that for a one-dimensional point source the group velocity is equal to<sup>9</sup>

$$G = x/t.$$

<sup>9</sup> See, for example, Lamb (1932, §241). For limitations of this formula, see Rossby (1945).

This formula is of great help in evaluating the phase distribution in a wave motion produced by a point source without entering into a detailed analysis of the motion (Rossby, 1945). Assuming the group velocity to be given uniquely by wave length  $L$  (or wave number  $k = 1/L$ ),

$$G = \varphi(k) = \varphi(\partial\psi/\partial x),$$

where  $k = \partial\psi/\partial x$  is the wave number and  $\psi$  the phase angle. Then, solving symbolically for  $\partial\psi/\partial x$ ,

$$\partial\psi/\partial x = \varphi^{-1}(x/t).$$

Thus, in principle,  $\psi$  can be found through integration if the function  $\varphi(k)$  is known.

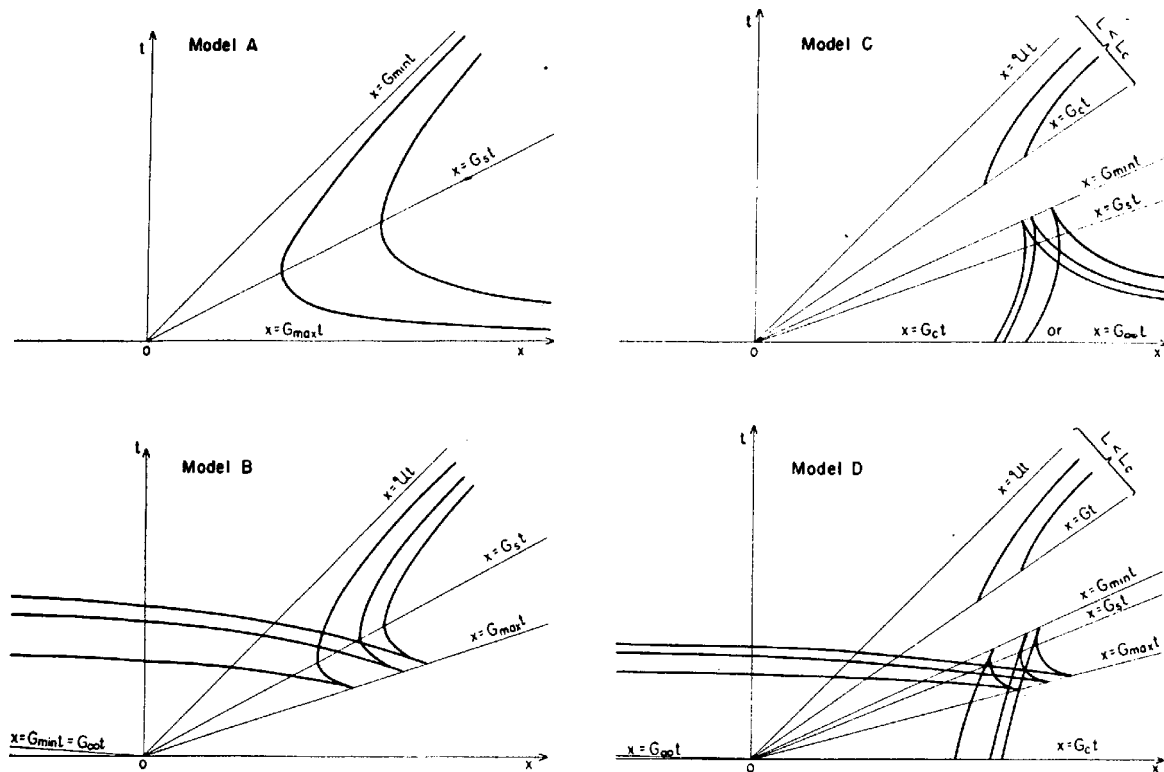


FIG. 7. Phase distribution in  $x, t$ -plane resulting from an instantaneous point-source disturbance. Upper left, model A; lower left, model B; upper right, model C (when the plus sign is taken in equation (3C)); lower right, model D (when the plus sign is taken in equation (3D)). The straight lines emanating from the origin are lines of constant group velocity  $G = x/t$ ; the curves are lines of equal phase. The values of the parameters used in constructing these diagrams are, in cgs units:  $f = 10^{-4}$ ,  $\beta = 1.60 \times 10^{-13}$ ,  $s = 5 \times 10^{-10}$ ,  $g = 10^3$ ,  $D_0 = 10^6$ .

However, the graphical method outlined below will serve to give a sufficiently accurate shape of the phase curves  $\psi(x, t) = \text{constant}$  in the  $x, t$ -plane due to a point-source disturbance. The region of disturbance by a point source will be confined between the two lines  $x = G_{\min}t$  and  $x = G_{\max}t$  where  $G_{\min}$  and  $G_{\max}$  are the minimum and maximum group velocities. Between these two lines are drawn the lines  $x = G_s t$ ,  $x = Ut$ ,  $x = G_\infty t$ , and  $x = G_c t$ , where  $G_s$  is the group velocity for  $L = L_s$  (the stationary wave length),  $U$  is the basic wind velocity,  $G_\infty$  the common limiting value of  $G$  and  $C$  as  $L \rightarrow \infty$ , and  $G_c$  the group velocity for  $L = L_c$  (the critical wave length). Since

$$C = \left( \frac{dx}{dt} \right)_\psi = - \frac{\partial \psi / \partial t}{\partial \psi / \partial x},$$

the curves  $\psi(x, t) = \text{constant}$  will start from the line  $x = G_{\min}t$  or  $x = G_{\max}t$  and have a slope<sup>10</sup> of  $C_{\min}^{-1}$  or  $C_{\max}^{-1}$ , where  $C_{\min}$  and  $C_{\max}$  are the phase velocities corresponding to  $G_{\min}$  and  $G_{\max}$ , respectively. The  $\psi$ -curves will cross the above four lines with a slope giving the proper phase velocity corresponding to the group velocities  $G_s$ ,  $U$ ,  $G_\infty$ , and  $G_c$ , respectively. If these characteristic lines do not provide sufficiently accurate shapes of  $\psi$ -curves we may draw any number

<sup>10</sup> The phase diagrams are plotted with  $x$  as abscissa and  $t$  as ordinate.

of auxiliary lines  $x = Gt$ . Then the  $\psi$ -curves will cross these lines with a slope of  $C^{-1}$ ,  $C$  being the phase velocity corresponding to  $G$ .

The characteristic values of the wave length, group velocity, and wave velocity used for the construction of the  $\psi$ -curves have been given in section 2. For the atmospheric models C and D two branches of waves are considered, one branch with wave length smaller than the critical value  $L_c$  and the other with wave length larger than  $L_c$ . (For the latter branch two cases, corresponding respectively to the positive sign and negative sign in (3C) and (3D), may be distinguished.)

With these characteristic values of the wave length, group velocity, and wave velocity, the  $\psi$ -curves resulting from a point-source disturbance in the four different models are constructed by means of the graphical method just described.

**Model A.**—In fig. 7 (upper left) the  $\psi$ -curves approach asymptotically to two lines parallel respectively to the lines  $x = Ut$  and  $t = 0$ . The slope of the  $\psi$ -curves changes sign along the line  $x = 2Ut$ ; this implies retrogressive waves in the region to the right of  $x = 2Ut$  and progressive waves in the region to the left of this line.

**Model B.**—In this model the region of disturbance is between  $x = G_{\min}t = G_\infty t$  and  $x = G_{\max}t$ . Since between the values  $U$  and  $G_{\max}$  each value of the

group velocity corresponds to two values of the wave length and wave velocity, at each point between the two lines  $x = Ut$  and  $x = G_{max}t$  there exist two wave trains of different wave length and wave velocity.

Let us first consider the branch of waves with wave length from 0 to  $(\lambda\sqrt{3})^{-1}$  (the wave length corresponding to  $G_{max}$ ). These waves will disturb only the region between  $x = Ut$  and  $x = G_{max}t$ . The  $\psi$ -curves, for this branch of waves, approach asymptotically a line parallel to  $x = Ut$  and the slope changes sign along the line  $x = G_s t$  so as to give progressive waves above this line and retrogressive waves below it (fig. 7, lower left). The  $\psi$ -curves cut the line  $x = G_{max}t$  with a slope of value  $C_{max}^{-1}$ . The second branch of waves, *i.e.*, from  $(\lambda\sqrt{3})^{-1}$  to  $L \rightarrow \infty$ , will be felt in the whole disturbed region. Since this branch consists only of retrogressive waves, the family of  $\psi$ -curves caused by this branch does not change slope and approaches asymptotically a line parallel to  $x = G_{min}t = G_x t$ . The two sets of  $\psi$ -curves are tangent to each other (cusped) along the line  $x = G_{max}t$ . From fig. 7 (lower left) it is seen that between  $x = G_{max}t$  and  $x = G_s t$  the two wave trains are progressive, and between  $x = G_s t$  and  $x = Ut$  one wave train is retrogressive and the other is progressive. In the rest of the disturbed region, there is only one wave train, retrogressive.

**Model C.**—In this model we must separate two branches of waves, one branch with wave length smaller than the critical wave length  $L_c$  and the other with wave length larger than  $L_c$ . The first branch of waves disturbs only the region between the two lines  $x = Ut$  and  $x = G_s t$ . The  $\psi$ -curves in this region approach asymptotically a line parallel to  $x = Ut$  and cut the line  $x = G_s t$  with a slope of  $C_c^{-1}$ .

For  $L > L_c$  there are two or three possible solutions depending on whether one takes positive, negative, or both signs in equation (3C). We shall consider the positive sign only. The region disturbed by this branch of waves is from the  $x$ -axis to the line  $x = G_{min}t$ . Within this region there exist two wave trains at each point because one value of group velocity corresponds to two wave lengths (fig. 7, upper right).

Considering the waves with wave length from  $L_c$  to  $2L_c/\sqrt{3}$  (the wave length corresponding to  $G_{min}$ ) the  $\psi$ -curves start from the  $x$ -axis (since  $G = \infty$  for this case) with a slope of  $C_c^{-1}$ , cutting the line  $x = G_s t$  with infinite slope (since  $C = 0$  along this line) and finally end on the line  $x = G_{min}t$  with a slope  $C_{min}^{-1}$ .

The other branch of waves, of wave length from  $2L_c/\sqrt{3}$  to  $\infty$ , gives another set of  $\psi$ -curves which is tangent to the first set at the line  $x = G_{min}t$  and asymptotically approaches a line parallel to the  $x$ -axis, so as to give an infinite phase velocity as  $L \rightarrow \infty$ .

From fig. 7 (upper right) we can see that between  $x = Ut$  and  $x = G_s t$  there is only one progressive wave train of short wave length; between  $x = G_{min}t$

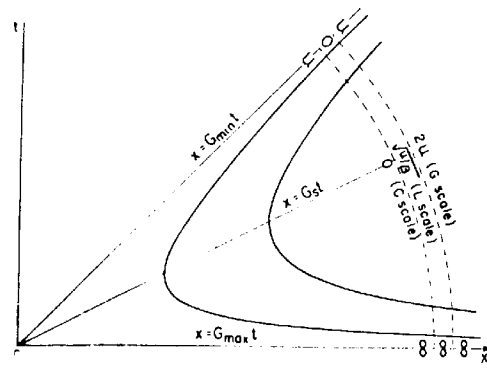


FIG. 8. Distribution of group velocity, phase velocity, wave length, and phase angle in  $x, t$ -plane resulting from an instantaneous point-source disturbance in model A. Along the circular arc the inner scale is for measurement of the phase velocity, the central scale for the wave length, and the outer scale for the group velocity.

and  $x = G_s t$  there are two wave trains, both retrogressive; and between  $x = G_s t$  and the  $x$ -axis there are also two wave trains, one progressive and the other retrogressive. The region between  $x = G_s t$  and  $x = G_{min}t$  is left undisturbed.

**Model D.**—In this atmospheric model waves are also branched into two groups at the critical wave length  $L_c$ . Taking the positive sign in (3D) we obtain fig. 7 (lower right) for the phase distribution. The region disturbed by a point-source is between the  $x$ -axis and  $x = G_s t$ . From fig. 5 we may pick out seven characteristic values of group velocity, namely  $U, G_c, \infty, G_{min}, G_s, G_{max},$  and  $G_\infty$ . Corresponding to these seven values of the group velocity there are seven characteristic lines shown in fig. 7 (lower right). Between the  $x$ -axis and  $x = G_{max}t$  there is one progressive wave train with almost uniform phase velocity since the phase velocity varies very little within this range of group velocity. From  $x = G_{max}t$  to  $x = G_{min}t$  there are three wave trains because one group velocity corresponds to three wave lengths; above the line  $x = G_s t$  two of the three wave trains are progressive and one is retrogressive while below this line two are retrogressive and one is progressive. Between the lines  $x = G_s t$  and  $x = Ut$  there are two wave trains, one progressive and one retrogressive. In the rest of the disturbed region there exists only one retrogressive wave train.

Combining the diagram for  $C$  and  $G$  with that for  $\psi(x, t)$  we may construct a single diagram containing all the four quantities  $L, C, G,$  and  $\psi(x, t)$ . Take the first model as an example. In the  $x, t$ -plane draw between the  $x$ -axis and  $x = Ut$  an arc with the origin of the  $x, t$ -plane as center (fig. 8). Three scales are laid off along this arc to measure the three quantities  $C, G,$  and  $L$ . In fig. 8 the innermost scale along the arc is for  $L$ , the central scale is for  $G$ , and the outermost scale is for  $C$ . Along each radius vector  $C, G,$  and  $L$  are constant. The three radii in fig. 8 serve as ex-

amples: along the radius  $x = Ut$ , the phase velocity and group velocity are the same and equal to  $U$ ; the wave length is 0. Along  $x = 2Ut$  the phase velocity is zero, the group velocity is  $2U$ , and the wave length is  $\sqrt{U/\beta}$ . Along the  $x$ -axis the phase velocity is  $-\infty$ , group velocity is  $+\infty$ , and wave length is  $+\infty$ . The curved lines are the phase curves  $\psi(x, t) = \text{constant}$ . In this diagram we have everything required to describe a wave motion except the amplitude. For the case when one group velocity is applicable to two different wave lengths the diagram will be slightly more complicated. In such a case we should have, for this range of group velocities, two scales for phase velocity and wave length because in this range there are two wave trains of different phase velocity and different wave length passing each point.

#### 4. Formation of a new trough downstream from a region of cyclogenesis

Through the effect of the earth's rotation, the atmosphere and oceans become dispersive media, *i.e.*, wave velocities in these media are functions of the wave length. In his study of the dynamics of the tide on the north Siberian shelf, Sverdrup (1927) established the existence of dispersive waves in the ocean. If dispersion is also an important process operating in the atmosphere its effect should be observed in our daily synoptic charts.

As a first application of the foregoing theory we shall discuss the formation of a new trough downstream from a region of cyclogenesis. A brief account of this investigation has already been given elsewhere (University of Chicago, 1947). It will be reproduced here in more detail.

It has been observed that when a deep trough is formed in the Gulf of Alaska its effects are almost immediately reflected downstream. The chain of events established downstream after this new trough formation, appears much faster than could be accounted for advectively by means of the prevailing wind speeds. Indeed, the effects of this cyclogenesis are not limited to its vicinity; correlated changes in the circulation over Europe have been observed. Namias (1944) explains this phenomenon by the shortening of wave length due to the formation of a new trough; but how this new trough is formed and why it is formed needs theoretical study.

Assume a barotropic atmosphere with a uniform basic west-wind current and nondivergent motion (model A). Beginning at a time  $t = 0$  cyclonic relative vorticity is injected at a constant rate at a prescribed longitude ( $x = 0$ ). Then our problem is to solve the vorticity equation

$$\frac{\partial^2 v}{\partial x \partial t} + U \frac{\partial^2 v}{\partial x^2} + \beta v = 0,$$

under the conditions

$$\begin{aligned} v &= 0, & \text{at } t &= 0 \\ v &= 0, & \partial v / \partial x &= \zeta_0 = \text{constant, at } x = 0. \end{aligned}$$

This problem, which can be solved by Riemann's method, has the solution

$$v(x, t) = \zeta_0 U \int_{t-x/U}^t J_0(\sqrt{4\beta(t-\theta)[x-U(t-\theta)]}) d\theta. \quad (5)$$

Since vorticity is injected beginning at time  $t = 0$  we must have  $(\partial v / \partial x)_0 = 0$  for  $t < 0$ . Therefore, when  $x > Ut$ , the lower limit of the above integral must be replaced by zero.

The physical meaning of (5) may be stated as follows: The disturbance produced at any point  $x$  at time  $t$  depends only on the disturbance prescribed at the source region (*i.e.*,  $x = 0$ ) from time  $t - x/U$  up to  $t$ ; in other words, the disturbance prescribed at  $x = 0$  from the time  $t = 0$  up to the time  $t_1 - x_1/U > 0$  will not have an effect on the region

$$x < Ut - U(t_1 - x_1/U).$$

It can readily be seen from (5) that a steady solution exists in the region  $x \leq Ut$ . Putting  $t - \theta = \tau$  and the lower limit equal to zero in (5) we have

$$v(x, t) = \zeta_0 U \int_0^{x/U} J_0(\sqrt{\beta U^{-1} x^2 [1 - (2Ux^{-1}\tau - 1)^2]}) d\tau,$$

which may, without much difficulty, be shown to reduce to

$$v(x, t) = \zeta_0 k^{-1} \sin kx, \quad \text{for } x \leq Ut, \quad (6)$$

where  $k \equiv \sqrt{\beta/U}$ . Along the line  $x = 2Ut$  we also have a steady solution, since in this case (5) reduces to

$$v(x, t) = \frac{1}{2} \zeta_0 k^{-1} \sin kx, \quad \text{for } x = 2Ut. \quad (7)$$

Equation (5) is difficult to integrate for  $x > Ut$ . However, approximations can be made in the region very remote from the line  $x = Ut$  or very near to it. When  $x \approx Ut$  we may integrate (5) by two steps as follows:

$$v(x, t) = \zeta_0 U \int_0^{x/U} J_0(\psi) d\theta + \zeta_0 U \int_{x/U}^t J_0(\psi) d\theta,$$

where  $\psi \equiv \sqrt{4\beta(t-\theta)[x-U(t-\theta)]}$ . The first integral has been found to be  $\zeta_0 k^{-1} \sin kx$ . To evaluate the second integral let  $kxp \equiv \psi$ ; then

$$\zeta_0 U \int_{x/U}^t J_0(\psi) d\theta = -\frac{1}{2} \zeta_0 x \int_0^P p(1-p^2)^{-1} J_0(kxp) dp,$$

where  $P \equiv 2x^{-1} \sqrt{Ut(x-Ut)}$ . Since very near the line  $x = Ut$ ,  $P$  is very small,  $(1-p^2)^{-1}$  may be

replaced by  $1 + \frac{1}{2}p^2$  approximately. Thus (5) becomes

$$v(x, t) \approx \zeta_0 k^{-1} \sin kx - \frac{1}{2}(1 + \frac{1}{2}P^2)\zeta_0 k^{-1} P J_1(kxP) + \frac{1}{2}\zeta_0 k^{-2} x^{-1} P^2 J_0(kxP), \quad (8)$$

when  $x \approx Ut$ .

Very far from the line  $x = Ut$ , in particular when  $x \gg 2Ut$ , (5) may be written as

$$v(x, t) = \frac{1}{2}\zeta_0 \alpha \int_0^P p(1 - p^2)^{-\frac{1}{2}} J_0(kxp) dp,$$

where  $P$  is small; we find then approximately

$$v(x, t) \approx \frac{1}{2}(1 + \frac{1}{2}P^2)\zeta_0 k^{-1} P J_1(kxP) - \frac{1}{2}\zeta_0 k^{-2} x^{-1} P^2 J_0(kxP), \quad (9)$$

when  $x \gg 2Ut$ .

Near the line  $x = 2Ut$  we may also obtain an approximate formula for (5). For this case we first integrate (5) from  $\theta = 0$  to  $\theta = x/2U$  and then from  $x/2U$  to  $t$ . The first integration gives  $\frac{1}{2}\zeta_0 k^{-1} \sin kx$  and the second integration gives

$$\pm \frac{1}{2}\zeta_0 \alpha \int_P^1 p(1 - p^2)^{-\frac{1}{2}} J_0(kxp) dp.$$

The plus sign is to be taken when  $x > 2Ut$  and the minus sign when  $x < 2Ut$ . Near the line  $x = 2Ut$  it can be seen that  $P$  is nearly equal to 1. Hence  $J_0(kxp)$  does not vary much in the interval of integration and can be taken out of the integral sign approximately. The solution for (5) is then

$$v(x, t) \approx \frac{1}{2}\zeta_0 k^{-1} \sin kx - \frac{1}{2}\zeta_0 (x - 2Ut) J_0(kx), \quad (10)$$

for  $x \approx 2Ut$ .

To sum up: in the region  $x \leq Ut$  the steady solution (6) holds; on the line  $x = 2Ut$  another steady solution (7) exists; very near or remote from the line  $x = Ut$  the unsteady solutions (8) or (9) are approximately valid, and in the vicinity of the line  $x = 2Ut$  (10) is the approximate solution.

Two interesting features are to be noted in the foregoing analysis. First is the steady condition existing in the region  $x \leq Ut$ . This steady solution is not surprising, as the nature of our boundary conditions will certainly lead to an equilibrium. But the interesting thing is that the steady motion starts from the time  $t = x/U$ , i.e., the time required for the particle to travel from the source of the disturbance to the region in question. From the constant-vorticity theory, the air particle brings with it the vorticity given to it at the source region. Hence, after the time  $t = x/U$  the air particles passing through the point  $x$  will have the same vorticity as that injected at  $x = 0$ . Another interesting feature is the steady solution along  $x = 2Ut$  which suggests that waves on the two sides of this line travel in opposite directions.

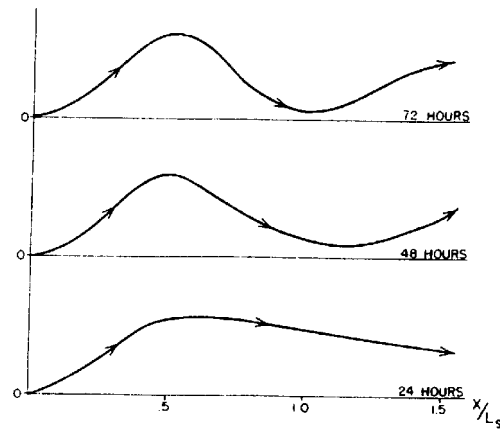


FIG. 9. Theoretical streamlines illustrating the establishment of a new wave in a straight zonal current as a result of the injection of cyclonic vorticity at a prescribed latitude.

Coming to the numerical computation, the method of numerical integration has been used in the regions where no approximate formula is available. Since these regions are to the right of  $x = Ut$ , zero is used for the lower limit of integral (5) which is for convenience written as

$$v(x, t) = \zeta_0 \int_0^{Ut} J_0(2k\sqrt{\varphi(x - \varphi)}) d\varphi$$

For convenience  $U$  is taken as 1000 km per day ( $11.6 \text{ m sec}^{-1}$ ) and a value of  $\beta$  at 45 degrees latitude is used ( $\beta = 1.62 \times 10^{-13}$  in cgs units). The results of computations for three successive days after injection of vorticity are summarized in the three streamline curves (in nondimensional units) of fig. 9.

The events illustrated by these computed streamlines have been observed repeatedly, namely the establishment of a ridge immediately east of the source of cyclogenesis, followed or accompanied by the development of a second ridge still farther to the east, with a new trough developing between these two ridges. For synoptic examples of this process, reference may be made to the University of Chicago study (1947, figs. 14 and 15), and to a recent paper by Cressman (1948, fig. 18).

The physical interpretation of this phenomenon is quite simple. As soon as the genesis of vorticity appears, the air particles start moving northward. To balance the Coriolis force set up by this northward motion there must be a pressure rise to the right, which will set the air farther to the east into motion.

The ideal conditions (uniform atmosphere and non-divergent motion) imposed upon the above analysis are perhaps too far from reality. We shall now investigate the effects of divergence and solenoids on this problem. Taking divergence into consideration first, the differential equation to be solved is equation (2B), which may be written in the following nondimensional

form:

$$\frac{\partial^3 v}{\partial \xi^2 \partial \tau} + \frac{\partial^3 v}{\partial \xi^3} + \frac{\partial v}{\partial \xi} - A^2 \frac{\partial v}{\partial \tau} = 0,$$

where  $\xi \equiv kx$ ,  $\tau \equiv t\sqrt{\beta U}$ , and  $A^2 \equiv f^2 U/gD_0\beta$ . The initial and boundary conditions are:

$$v = 0, \quad \frac{\partial v}{\partial \xi} = \zeta_0, \quad \frac{\partial^2 v}{\partial \xi^2} = 0, \quad \text{for } \xi = 0 \\ v = 0, \quad \text{for } \tau = 0 \quad \text{and} \quad \xi > 0.$$

The problem is easily treated by the method of Laplace transformation.<sup>11</sup> Writing  $\nu^2 \equiv 2(1 + A^2)\tau^2$  the solution is

$$v(\xi, \tau) = \zeta_0 \sin \xi + v_1(\xi, \tau) + v_2(\xi, \tau), \quad (11)$$

where, for  $\xi > \tau$ ,

$$v_1(\xi, \tau) \equiv -\zeta_0 e^{A(\xi-\tau)} \int_0^{\xi-\tau} e^{-2Am} J_0(\nu\sqrt{m}) \\ \times J_0(\nu\sqrt{\xi-\tau-m}) dm \\ v_2(\xi, \tau) \equiv \zeta_0(1 + A^2) \int_0^{\xi-\tau} e^{An} \sin(\xi - \tau - n) \\ \times \int_0^n e^{-2Am} J_0(\nu\sqrt{n-m}) dm dn,$$

and for  $\xi < \tau$ ,

$$v_1(\xi, \tau) \equiv 0 \equiv v_2(\xi, \tau).$$

The motion is steady in the region  $\xi < \tau$  and the solution in this region is exactly the same as if the motion were nondivergent. The only difference the divergence makes is in the region  $\xi > \tau$ . The longer the time the larger the region unaffected by divergence. For this region the conclusions reached regarding the formation of a new trough in the nondivergent case, still hold here.

Considering nondivergent motion in an atmosphere with horizontal solenoids we use equation (2C) which is

$$\frac{\partial^3 v}{\partial \xi^2 \partial \tau} + 2 \frac{\partial^3 v}{\partial \xi^2 \partial \tau} + \frac{\partial^3 v}{\partial \xi^3} + \frac{\sigma}{\beta} \frac{\partial v}{\partial \tau} + \frac{\partial v}{\partial \xi} = 0,$$

in nondimensional variables. To solve the same problem we have the following conditions:

$$v = 0, \quad \frac{\partial v}{\partial \xi} = \zeta_0, \quad \frac{\partial^2 v}{\partial \xi^2} = 0, \quad \text{for } \xi = 0 \\ v = 0, \quad \frac{\partial v}{\partial \tau} = 0, \quad \text{for } \tau = 0.$$

Using again the method of Laplace transformation we

<sup>11</sup> See, for example, Carslaw (1941). To obtain the solution in the form given by (11), the Laplace transform of the function  $v(\xi, \tau)$  has been arranged in the form

$$v(p) = -\zeta_0 \left(1 - \frac{1 + A^2}{1 + p^2}\right) \frac{1}{p - A} e^{-\frac{\nu^2/4}{p-A}} \frac{1}{p + A} e^{-\frac{\nu^2/4}{p+A}} \\ + \zeta_0 (1 + p^2)^{-1},$$

where  $\nu^2 \equiv 2(1 + A^2)\tau^2$ .

may show that our solution in region  $\xi < \tau$  is<sup>12</sup>

$$v(\xi, \tau) = \zeta_0 \sin \xi.$$

This gives exactly the same streamlines in the region  $\xi < \tau$  as if solenoids were not operating. The solenoidal effect as well as the effect of divergence is present only in the region  $\xi > \tau$ .

The foregoing analysis shows that neither divergence nor solenoids essentially modifies the picture obtained without them. However, it remains to be shown whether the combined effect of divergence and solenoids would produce important changes. When both divergence and solenoids are present equation (2D) is used, in non-dimensional form:

$$\frac{\partial^4 v}{\partial \xi^2 \partial \tau^2} + 2 \frac{\partial^4 v}{\partial \xi^3 \partial \tau} + \frac{\partial^4 v}{\partial \xi^4} - A^2 \frac{\partial^2 v}{\partial \tau^2} + \frac{b}{\beta} \frac{\partial^2 v}{\partial \xi \partial \tau} + \frac{\partial^2 v}{\partial \xi^2} = 0.$$

The conditions to be satisfied are

$$v = 0, \quad \frac{\partial v}{\partial \xi} = \zeta_0, \quad \frac{\partial^2 v}{\partial \xi^2} = 0, \quad \frac{\partial^3 v}{\partial \xi^3} = -\zeta_0, \quad \text{for } \xi = 0 \\ v = 0, \quad \frac{\partial v}{\partial \tau} = 0, \quad \text{for } \tau = 0.$$

The presence of the additional boundary condition ( $\partial^2 v/\partial \xi^2 = -\zeta_0$ ) may be explained as follows:

The above differential equation is derived through the elimination of  $q$  from the following two equations:

$$\frac{\partial^3 v}{\partial \xi^2 \partial \tau} + \frac{\partial^3 v}{\partial \xi^3} + \frac{\partial v}{\partial \xi} + fk \frac{\partial^2 q}{\partial \xi \partial \tau} - A^2 \frac{\partial v}{\partial \tau} = 0 \\ \frac{\partial q}{\partial \tau} + \frac{\partial q}{\partial \xi} = \frac{sv}{\sqrt{\beta U}}.$$

At  $x = 0$  all but two of the terms of the first equation are zero. The two nonvanishing terms,  $\partial^3 v/\partial \xi^3$  and  $\partial v/\partial \xi$ , should balance each other. If  $\partial v/\partial \xi = \zeta_0$ , then  $\partial^3 v/\partial \xi^3 = -\zeta_0$ .

Using the same method as employed before, we have

$$v(\xi, \tau) = \zeta_0 \sin \xi, \quad \text{for } \xi < \tau,$$

which is exactly the same as in each of the preceding cases.

The foregoing analysis thus shows a steady-state motion in the region  $\xi < \tau$  in each of the models considered. Physically the appearance of this steady-state motion is a natural consequence of the imposed boundary conditions. Since the relative vorticity is injected at a constant rate at a fixed point a steady-state motion should appear at each point after a

<sup>12</sup> The Laplace transform of  $v$  may be expressed as

$$v(p) = \zeta_0(1 + p^2)^{-1} + e^{-p\tau} \times \{\text{terms involving } p \text{ and } \tau\}.$$

The transform of  $\zeta_0(1 + p^2)^{-1}$  is  $\zeta_0 \sin \xi$ , while the transform of the remaining terms vanishes when  $\xi < \tau$  because of the presence of the factor  $e^{-p\tau}$ .

sufficiently long time. In a steady-state motion stream lines and isotherms are parallel (Rossby, 1942) so the solenoids vanish; convergence is likewise absent in the steady region  $\xi < \tau$ . Thus the absolute vorticity is propagated advectively and a steady motion follows.

**5. Dispersion of an initial solitary wave; the blocking action and the intensity of disturbances at different latitudes**

One of the most remarkable phenomena and at the same time a very useful tool in forecasting is the so-called "blocking" effect, first noted by Garriott (1904) and later discussed in more detail by Namias (1947) and by Elliott and Smith.<sup>13</sup> As described by Namias (1947), blocking is associated with a retardation in the zonal circulation, which progresses slowly westward. For example, the diminution in the strength of the westerlies usually first in evidence over Europe or the eastern Atlantic, is observed to proceed slowly westward to the western Atlantic, North America, the Pacific, and sometimes westward into Siberia. The decline in circulation proceeds westward and is accompanied by an increase in mass of air, that is, by westward progress of an area of pressure rise. A striking example of blocking was given by Namias (1947). The details of the blocking mechanism are still obscure. In the following an interpretation will be advanced.

In section 2 of this paper it was shown that in a uniform atmosphere of finite depth the group velocity is negative above a certain wave length. This means that part of the energy will be dispersed upstream. This upstream propagation of energy may be related to blocking.

Assume that initially the atmosphere is undisturbed with a basic current of constant west wind. Due to some process, at time  $t = 0$  part of the free surface is lifted so that there is a pressure rise in that area. The subsequent development of this pressure rise will be investigated. Denoting the deformation of the free surface by  $D'$ , which is a measure of pressure change, we have the following nondimensional equation in  $D'$  obtained from equation (2B):

$$\frac{\partial^3 D'}{\partial \xi^2 \partial \tau} + \frac{\partial^3 D'}{\partial \xi^3} + \frac{\partial D'}{\partial \xi} - A^2 \frac{\partial D'}{\partial \tau} = 0,$$

where  $A^2 \equiv f^2 U / g D_0 \beta$  and  $D_0$  is the initial depth, uniform with respect to  $\xi$ . Assume an initial solitary wave to be represented by

$$D'(\xi, 0) \equiv \frac{1}{2} B \sqrt{\pi} a^{-1} e^{-\xi^2 / 4a^2},$$

where  $a^2$  is an arbitrary nondimensional constant, and  $B$  any other constant of dimension of length. Then at any subsequent time,  $D'(\xi, \tau)$  can be determined from the following integral:

$$D'(\xi, \tau) = B \int_0^\infty e^{-a^2 k^2} \cos \left( k\xi - \tau \frac{k^3 - k}{A^2 + k^2} \right) dk. \quad (12)$$

Unfortunately this integral is difficult to evaluate algebraically. However, because of the presence of the exponentially decreasing factor  $e^{-a^2 k^2}$  it is not difficult to evaluate numerically.

Since  $A^2$  depends on latitude the dispersion should be a function of latitude. To illustrate this effect, the integral in (12) has been evaluated numerically for three different latitudes: 70°, 40°, and 0°. We may note that at the pole the basic zonal current  $U$  must decrease to zero. However, if one could maintain a finite zonal current  $U$  near the pole, then  $A^2 \sim \sec \phi \rightarrow \infty$  at the pole and (12) becomes

$$D'(\xi, \tau) = B \int_0^\infty e^{-a^2 k^2} \cos k\xi dk = \frac{1}{2} B a^{-1} \sqrt{\pi} e^{-\xi^2 / 4a^2}.$$

This equation shows that once a pressure rise or fall is formed near the pole it would remain there without being dispersed. This would correspond to an extremely slowly moving blocking wave.

At the equator, equation (12) reduces to

$$D'(\xi, \tau) = B \int_0^\infty e^{-a^2 k^2} \cos [k\xi + \tau(k^{-1} - k)] dk. \quad (13)$$

There is a difficulty in evaluating this integral near  $k = 0$ . As  $k \rightarrow 0$  the argument of the cosine becomes infinite. A slight increase in  $k$  produces a large variation in the argument. Thus the cosine term will oscillate very rapidly near  $k = 0$ . Therefore, the integrand in the range near  $k = 0$  will not contribute very much to the value of the final result. However, the contribution of this range near  $k = 0$  will be estimated. In evaluating the above integral the interval of integration is divided into two parts, one from  $k = 0$  to 0.2, and the other for  $k > 0.2$ . For the first interval the integral (13) may be written:

$$\int_0^{0.2} e^{-a^2 k^2} [\cos k(\xi - \tau) \cos k^{-1} \tau - \sin k(\xi - \tau) \sin k^{-1} \tau] dk.$$

Expanding  $e^{-a^2 k^2} \cos k(\xi - \tau)$  and  $e^{-a^2 k^2} \sin k(\xi - \tau)$  into power series in  $k$  (since  $k$  is very small for the whole range of integration, terms of higher degree than  $k^3$  are neglected), the general term of the integrand is of the form  $y^{-n} \cos y$  or  $y^{-n} \sin y$ , where  $y = \tau/k$ . These terms can be integrated by parts; for example, when  $n = 2$ ,

$$\int y^{-2} \cos y dy = -y \cos y - \int y^{-1} \sin y dy,$$

<sup>13</sup> R. D. Elliott and T. B. Smith, "A study of the effects of large blocking highs on the general circulation in the northern hemisphere westerlies," 1948 (to be published in this JOURNAL).

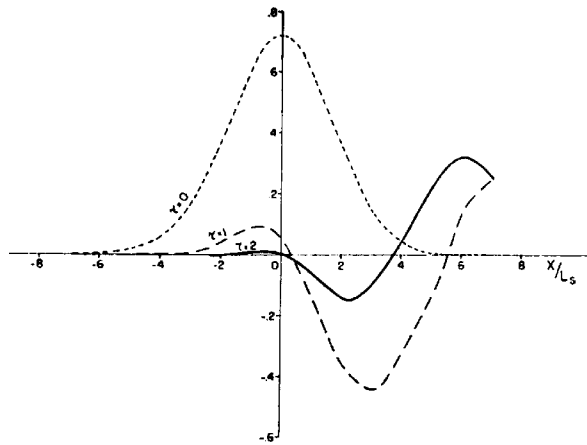


FIG. 10. Dispersion of an initial solitary wave ( $\tau = 0$ ) at the equator. The dashed line ( $\tau = 1$ ) is the wave profile after approximately 18.4 hours, and the solid line ( $\tau = 2$ ) after approximately 36.8 hours.

the last term of which is the sine integral and tabulated.

For the second interval ( $k > 0.2$ ) of (13) ordinary methods of numerical integration are used. The results of the calculation are given in fig. 10. In this computation  $a^2$  is taken as 1.5. The dotted curve is for  $\tau = 0$  (the initial solitary wave), the dashed curve is for  $\tau = 1$ , and the solid curve for  $\tau = 2$ . At the equator  $\tau = 1$  corresponds to 18.4 hours approximately, if  $U = 10 \text{ m sec}^{-1}$ . We see from the curves that after 18.4 hours the high pressure is reduced to about 1/7 of its initial value and after about 36.8 hours it disappears entirely. It is also to be noted in fig. 9 that the center of high pressure is shifted westward.

In middle latitudes the value of  $A^2$  is finite and positive. Hence, a solitary wave formed in middle latitude would travel westward and at the same time would spread out and be dispersed. Since at the pole the wave would remain where it was formed, we may infer that the speed of westward retrogression decreases with increasing latitude. Since at the pole its intensity would remain constant the rate of its dispersion decreases with increasing latitude.

To verify these statements two computations were made, one at latitude  $40^\circ\text{N}$  and one at  $70^\circ\text{N}$ . For both cases a value of  $17 \text{ m sec}^{-1}$  is used for  $U$ , and 8 km for  $D_0$ . Fig. 11 is for  $40^\circ\text{N}$  and fig. 12 for  $70^\circ\text{N}$ . In both figures the dotted curve is for  $\tau = 0$  (the initial solitary wave), the dashed curve is for  $\tau = 1$ , and the solid curve for  $\tau = 2$ . At  $40^\circ\text{N}$ ,  $\tau = 1$  is approximately 16 hours while at  $70^\circ\text{N}$   $\tau = 1$  is approximately one day. The abscissae of these curves are in units of  $\sqrt{U/\beta}$  which is equal to 1000 km approximately in fig. 10 and equal to 2200 km approximately in fig. 11. From fig. 10 it is seen that the center of the initial high pressure at  $40^\circ\text{N}$  moves approximately 800 km in the first 16 hours, or 1200 km per day, with its central pressure diminished by about 1/7 of its initial value.

However, in the next 16 hours it rapidly moves westward. Indeed, it is difficult to locate the high center after 36 hours; it is near  $\xi = -6$  or 6000 km west of its initial position at the end of 32 hours, corresponding to a speed of approximately 7500 km per day in the second 16 hours. Further, its intensity is greatly reduced. In comparison, the solitary wave at  $70^\circ\text{N}$  is not dispersed very much. In the first day the center of the wave moves from  $\xi = 0$  to about  $\xi = -0.4$ , with a speed of approximately 880 km per day. The central pressure is reduced by about only four per cent. At the end of the next day ( $\tau = 2$ ) the center is located at about  $\xi = -0.8$  or 1760 km to the west of its original position. Its speed of retrogression in the second day is exactly equal to that in the first day, not as in the case of  $40^\circ\text{N}$  where the retrogression is accelerated. Its central pressure at the end of the second day is, however, diminished by about 1/7 of its original value.

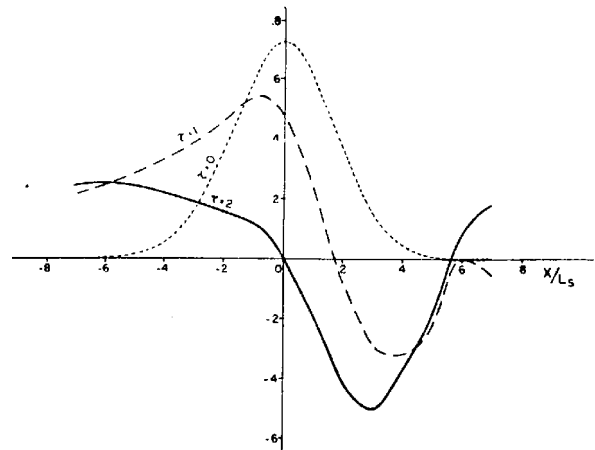


FIG. 11. Dispersion of an initial solitary wave ( $\tau = 0$ ) at 40 degrees latitude. The dashed line ( $\tau = 1$ ) is the wave profile after approximately 16 hours and the solid line ( $\tau = 2$ ) after approximately 32 hours.

It is a matter of experience that the blocking waves are usually observed at high latitudes. In lower latitudes they are scarcely noticed. The reason for this is very obvious from the computations. In low latitudes they are dispersed so quickly that we are not able to detect them. Even around 40 degrees latitude their life-time is not longer than two days, as can be seen from fig. 10.

In a recent report by Elliot and Smith,<sup>14</sup> blocking action is divided into low-latitude and high-latitude cases. The former include those blocking actions whose centers lie below  $57.5^\circ\text{N}$ . During their investigation period the frequency of the high-latitude class was higher than that of the low-latitude class. The average life of their high-latitude blocking actions was considerably longer than, indeed, more than double the lifetime of the low-latitude class. This

<sup>14</sup> See footnote 13.



observation supports our theoretical investigation. Unfortunately no data on the speed of the blocking wave are available. According to Namias (1947) it is about 60 degrees longitude per week. This is not too far from the calculated speed at 70°N.

To summarize the discussion in this section, we may make the following statements:

1. The blocking effect is a high-latitude phenomenon.
2. The intensity of the blocking wave increases with latitude.
3. The speed of the blocking wave decreases with latitude.
4. The lifetime of the blocking wave increases with latitude.

Another phenomenon which has no apparent relation with blocking action may be associated with it. It is a common experience that we do not observe large and strong perturbations in low-latitudes, in the lower troposphere at least. The intensity of large-scale disturbances generally decreases with decreasing latitude. In middle and high latitudes we have extratropical systems with large ridges and intense troughs. In the subtropical easterlies, we observe mainly easterly waves with much smaller intensity than the extratropical systems. In equatorial latitudes even the easterly waves are rare. The current over the equator is generally undisturbed except when occasionally interrupted by a current from the southern hemisphere. This reduction of the intensity of the disturbances with latitude could be associated with the increase in solenoidal intensity with latitude, but the small value of the Coriolis parameter in the tropics would favor large systems in tropics. Another way to look at the problem is from the point of view of the lifetime of the disturbances. Once a disturbance is formed in one way or another it can persist a long time in middle or high latitudes, but dies out almost immediately over the equator, as shown in the above computations. Therefore unless there is a continuous

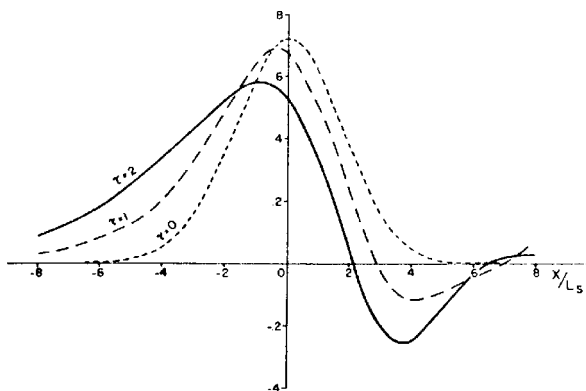


FIG. 12. Dispersion of initial solitary wave ( $\tau = 0$ ) at 70 degrees latitude. The dashed line ( $\tau = 1$ ) is the wave profile after approximately 1 day and the solid line ( $\tau = 2$ ) after approximately 2 days.

energy supply from a huge energy source there will not be a chance for a large-scale disturbance to persist long enough to be observed in low latitudes.

Another conclusion we can reach from our computation is that in divergent motion more energy is dispersed upstream while in nondivergent motion no energy will be transmitted upstream. In nondivergent motion there will be no deformation of the free surface. The same differential equations which describe this deformation  $D'$  also hold for  $v$ , the north-south component of disturbed velocity. The problem of dispersion of an initial meridional perturbation will have the same solution. We can simply use the results computed for  $D'$  to interpret  $v$ . It is then seen that our conclusion concerning the speed of energy propagation is correct. As a matter of fact this is simply a restatement that the group velocity in nondivergent motion is always positive while in divergent motion it may be negative.

One common feature among figs. 10, 11, and 12 is the downstream wave formation. At first, the amplitude of the newly formed wave increases with time at the expense of the initial solitary wave. This verifies, partly at least, the statement made in section 2: in nondivergent motion no energy will be available upstream. In divergent motion though the group velocity can be negative, *i.e.*, energy will be transmitted upstream, its magnitude is smaller than that of the phase velocity in the same direction. Hence, the energy transmitted upstream cannot overtake the retrogressing waves, so that only an increasingly long trailing wave train may develop upstream. On the other hand downstream energy propagation is more rapid than phase velocity, so that new waves will form.

From the foregoing analysis it can be stated that dispersion is a fundamental process operating in the atmosphere. Several frequently observed phenomena have been explained by it. It is believed that many other phenomena can also be interpreted by this process and further illustrations will be given in a later report.

*Acknowledgments.*—The author wishes to acknowledge the stimulating guidance of Prof. C.-G. Rossby without whose suggestions and encouragement this paper would never have been written. Sincere thanks are due to Dr. Z. Sekera for his criticisms and discussions. Discussion with Mr. H. L. Kuo has also been fruitful.

#### REFERENCES

- Cahn, A. Jr., 1945: An investigation of the free oscillations of a simple current system. *J. Meteor.*, **2**, 113-119.
- Carlsaw, H. S., 1945: *Mathematical theory of the conduction of heat in solids*. 2 ed., Dover Publications, New York, 268 pp.
- Charney, J., 1947: The dynamics of long waves in a baroclinic westerly current. *J. Meteor.*, **4**, 135-162.
- Cressman, G. P., 1948: On the forecasting of long waves in the upper westerlies. *J. Meteor.*, **5**, 44-57.

- Garriott, E. B., 1904: Long range forecasts. U. S. Weather Bureau Bulletin, No. 35.
- Haurwitz, B., 1940: The motion of atmospheric disturbances. *J. marine Res.*, **3**, 35-50.
- Jaw, J. J., 1946: The formation of semipermanent centers of action in relation to the horizontal solenoidal field. *J. Meteor.*, **3**, 103-114.
- Margules, M., 1905: Über die Energie der Stürme. *Jahrb. (Anh., 1903) Zentralanst. f. Meteor. Geodyn., Wien.* (English translation in "The mechanics of the earth's atmosphere. A collection of translations by Cleveland Abbe," *Smithson. misc. Coll.*, **51**, no. 4, 533-595, 1910).
- Namias, J., and Clapp, P. F., 1944: Studies of the motion and development of long waves in the westerlies. *J. Meteor.*, **1**, 57-77.
- Namias, J., 1947: *Extended forecasting by mean circulation methods.* Washington, U. S. Department of Commerce. Weather Bureau, 89 pp.
- Rossby, C.-G., 1936: Dynamics of steady ocean currents in the light of experimental fluid mechanics. *Pap. phys. Ocean. Meteor., Mass. Inst. Tech. & Woods Hole ocean. Instn*, **5**, no. 1, 43 pp.
- , 1937: On the mutual adjustment of pressure and velocity distributions in certain simple current systems, I. *J. marine Res.*, **1**, 15-28.
- , 1938: On the mutual adjustment of pressure and velocity distributions in certain simple current systems, II. *J. marine Res.*, **1**, 239-263.
- , 1942: Kinematic and hydrostatic properties of certain long waves in the westerlies. *Dep. Meteor. Univ. Chicago, Misc. Rep.*, no. 5, 75 pp.
- , 1945: On the propagation of frequencies and energy in certain types of oceanic and atmospheric waves. *J. Meteor.*, **2**, 187-204.
- , and collaborators, 1939: Relation between variations in the intensity of the zonal circulation of the atmosphere and the displacements of the semi-permanent centers of action. *J. marine Res.*, **2**, 38-55.
- Sverdrup, H. U., 1927: Dynamics of tides on the North Siberian shelf. *Geofys. Publ.*, **4**, no. 5, 75 pp.
- University of Chicago, Department of Meteorology, 1947: On the general circulation of the atmosphere in middle latitudes. *Bull. Amer. meteor. Soc.*, **28**, 255-280.